Controllable and reversible tuning of material rigidity for robot applications

Liyu Wang [1,*,†], **Yang Yang** [2,†], **Yonghua Chen** [2], **Carmel Majidi** [3], **Fumiya Iida** [4], **Erin Askounis** [5], **Qibing Pei** [5]

[1] Department of Electrical Engineering and Computer Sciences, University of California, Berkeley, USA
[2] Department of Mechanical Engineering, The University of Hong Kong, China
[3] Department of Mechanical Engineering, Carnegie Mellon University, USA
[4] Engineering Department, The University of Cambridge, UK
[5] Department of Materials Science and Engineering, University of California, Los Angeles, USA

Tunable rigidity materials have potentially widespread implications in robotic technologies. They enable morphological shape change while maintaining structural strength, and can reversibly alternate between rigid, load bearing and compliant, flexible states capable of deformation within unstructured environments. In this review, we cover a range of materials with mechanical rigidity that can be reversibly tuned using one of several stimuli (e.g. heat, electrical current, electric field, magnetism, etc.). We explain the mechanisms by which these materials change rigidity and how they have been used for robot tasks. We quantitatively assess the performance in terms of the magnitude of rigidity, variation ratio, response time, and energy consumption, and explore the correlations between these desired characteristics as principles for material design and usage.

Introduction

Traditionally in design and manufacturing, materials have been chosen with certain fixed mechanical properties that satisfy functional criteria and economic constraints defined by the application. Once these mechanical properties like elastic modulus, flexural rigidity, and strain limit are specified, they are not expected to change during the course of operation. However, emerging applications in medicine, structural engineering, vehicle design, aeronautics and aerospace, and consumer wearable electronics require materials with variable rigidity. For example, one of the uses of variable rigidity is in morphing structures that undergo dramatic changes in shape. For these applications, low rigidity is required to reduce mechanical resistance during shape change and high rigidity is required for structural load bearing after the shape change is complete. Another use is in wearable computing or robotic exoskeletons. During mechanically passive

operation or when being attached to the body, the material should be soft and compliant, conform to the skin, and not interfere with natural bodily motion. When stiffened, the material can keep computing hardware firmly fixed to the body or provide robotic assistance during motor tasks. Other potential applications of variable rigidity tuning include vibration and noise control in aerospace structures, insertion of soft biomechanically compatible needles for neural implants and drug delivery, and artificial muscle for soft bio-inspired robots.

Several terms have been used, but not necessarily accurately, in literature to refer to the same concept, i.e. "rigidity", "stiffness" or "elasticity". We use "rigidity" because it implies that a material is resistant to mechanical deformation everywhere (homogenous) and in every direction (isotropic). In contrast, "stiffness" can be directional and is sometimes defined for only a single loading direction (e.g. a material can be stiff in tension but not in torsion or flexure). Also, "elasticity" relates to a specific mode of deformation that is reversible and allows a solid to recover its original shape when load is removed. From an engineering point of view, variable rigidity can be achieved

* Corresponding author.
  E-mail address: Wang, L. (liyu.wang@wadh.oxon.org).
† These authors contributed equally to this work.

RESEARCH: Review

mechanically in macroscopic structures (or variable stiffness in this case). However, there is a trend to use materials whose intrinsic rigidity can be controlled in a reversible manner through electrical stimulation [1–3]. This allows for compatibility with miniaturizable electronics for control and power, and eliminates dependency on bulky external hardware for pneumatic, hydraulic, thermal, or magnetic stimulation.

This review focuses on materials with variable rigidity and tuning techniques for robotics applications. Historically, robotic systems have been primarily composed of rigid materials that have an elastic modulus over 1 GPa [4–6]. Metals, hard plastics, and hard composites are capable of supporting large forces but introduce mechanical constraints. Such mechanical constraints reduce a system's degrees of freedom (DOF) and ability to conform to surfaces in unstructured or irregularly shaped environments. Soft polymers, elastomers, and fluids have typically been avoided because they introduce deformations or changes in robot state that are difficult to monitor or anticipate, resulting in poor systems observability and controllability. Nonetheless, starting in the late 1940s, there has been interest in using soft materials and fabrics to create "artificial muscles" and since the late 1970s in soft-material robotic systems. Examples include the McKibben and Baldwin actuators, Bridgestone Rubbertuator, and inflatable soft robots created by Koichi Suzumori and colleagues at Okayama University and Toshiba R&D Center. More recently, there has been renewed interest in the so-called "soft robotics" from the perspective of materials science and chemistry [7,8]. These robots have shown mechanically compliant behaviors for adapting their shape in complex environments [4–6,8,9]. However, they do not have the force and torque output or load bearing properties of conventional piecewise-rigid robots.

As with biological organisms, robust movement and mechanical work output depend on materials that are not just compliant and deformable but also capable of rapidly tuning their rigidity, such as in mammalian muscles, echinoderm body [10], and fresh-water fish, etc. From the perspective of bioinspiration and biomimetics, variable rigidity materials should be useful for enhancing adaptability and increase robustness of a robotic system for multiple or unanticipated task environments. This is achievable in at least three ways. First, variable rigidity materials enable automatic morphological change in body structures [9], sensors [11] and even actuators of the robot. Second, they enable controllable stiffness variation of mechanical structures of the robot [3]. Third, they enable automatic modification of surrounding environments.

Here we cover a range of materials with mechanical properties (e.g. elastic modulus, viscosity) that are reversibly tunable. These materials have the potential to be used as artificial muscle or stiffness-varying tendons for a broad variety of robot applications. We review the underlying mechanisms for rigidity change and their influence on meso/macroscale properties. Furthermore, we propose additional materials and rigidity-tuning functionalities that could be explored in future research.

Variable-rigidity materials

Materials with variable rigidity can be intrinsically adaptive semi-active materials or active materials [1,2]. Intrinsically adaptive

materials undergo transformations in their molecular or microscopic structure in response to external stimuli and these changes affect their mechanical properties, hence they are semi-active. These usually include shape memory alloys (SMAs), shape memory polymers (SMPs), magnetorheological fluids (MRFs), low-melting-point alloys (LMPAs), thermoplastic elastomers (TPEs), and certain kinds of electroactive polymers (EAPs) such as electrorheological fluids (ERFs), liquid crystal elastomers (LCEs), and Electrochemo-mechanical conducting polymers (ECMCPs) etc. Active materials act as energy transducers, e.g. actuators or generators, to convert between the mechanical energy of deformation and the electrical (or thermal) energy that is used to modulate the properties. These generally include certain kinds of EAP, piezoelectric polymers (PZPs), ferromagnetic shape memory alloys (MSMAs), etc. Table 1 gives a list of materials that have shown variable rigidity experimentally. Some of the materials have already been used for rigidity tuning in robotics applications, in which case the related robot tasks are also listed.

For variable rigidity materials to be useful for various real-world applications, a number of desired characteristics have been proposed [1]. Most of them apply to robot applications: (i) rigidity tuning should be electrically controllable as robots are usually electromechanical systems; (ii) a high strength-weight ratio is essential because being lightweight and compact is important for mobile (legged, wheeled, flying) systems; (iii) the process requires low energy consumption, which is crucial for untethered robots with limited energy capacity; (iv) the process of rigidity change needs to be fast because robot systems can be highly dynamic; (v) a range of variable modulus of above 100 or even 1000-fold is necessary for robots that may morph their own structures or modify environments with limited actuator forces; (vi) the process shall be reversible and repeatable. In some robot tasks, large strain may be needed, however this is not always required and in many cases morphing can be a better solution. In addition, it is important that the induction technique only introduces minimal additional components and complexity into the system.

Depending on the method of stimulation for rigidity change, materials may be put into four categories: thermal, pressure, magnetic field, and electric field.

Thermal induced

Reversible variation of rigidity with thermal stimulation can be found primarily in thermoplastics. Thermoplastics have a melting temperature (T_m) and can also have a glass transition (T_g) between a crystalline or semi-crystalline phase and an amorphous rubbery phase. An example of glass transition is shown in Figure 2a, which shows atomic force microscopy (AFM) images of PCL-PIBMD50 and the transition from predominately rigid to soft amorphous domains during glass transition [52]. This change in microscopic structure contributes to a reduction in the elastic modulus measured at the macroscopic scale.

In general, rigidity tuning is possible within temperature ranges above, below, or across either T_g or T_m. Wang et al. used ethylene–vinyl acetate (EVA, $T_g = -20\ °C$) to enable dragline forming in a vertical mobile robot and movement on them

TABLE 1

Variable rigidity materials.

	Induction Method	Material Type	Components	Variable Rigidity Robot Applications
Intrinsic adaptive semi-active	Thermal	Thermoplastics (non SMPs)	Structural parts, actuator parts	Grasping, environment modification [12]
	Thermal	Shape memory polymers (SMPs) and composites	Joints, actuators	Grasping, manipulation [13,14]
	Thermal	Low melting point alloys (LMPAs)	Actuators, structural parts	Grasping, ladder climbing [15,16]
	Thermal	Wax	Structural parts	N/A
	Thermal	Conductive Thermoplastic elastomer (cTPE) [17]	Tendon [95,96]	Grasping [96]
	Thermal	Shape memory alloys (SMAs)	Actuators	N/A
	Thermal	Liquid crystal elastomers (LCE)*	N/A	N/A
	Pressure	Granular materials	Actuator parts, structural parts	Grasping, ground rolling, ground sliding [18]
	Pressure	Fluid-polymer composites	Actuator parts, structural parts	Load bearing [19]
	Magnetic field	MR fluids (MRF)	Clutches	Manipulation, haptic interface [20]
	Magnetic field	MR elastomers (MRE)	Dampers	Prosthetic device [21]
	Electric field	ER networks (ERN)	Dampers	N/A
	Electric field	ER fluids (ERF)*	Actuators, structural parts	Manipulation, ground crawling, haptic interface [22]
	Electric	Electroactive gel*	Actuators	Wearable assistive device [23]
	Electric	Electrochemo-mechanical conducting polymers (ECMCP)*	N/A	N/A
Active	Electric	Dielectric elastomers*	Actuators	N/A
	Thermal	Piezoelectric polymer (PZP)	N/A	N/A
	Thermal	Bistable EAPs*	Structural parts, actuator parts	N/A
	Magnetic field	Ferromagnetic SMAs (MSMA)	N/A	N/A

N/A: not available.
* Subset of electroactive polymers (EAPs).

immediately afterward [12]. They demonstrated the use of rigidity variation in on-the-fly formation of draglines with a diameter of 1.17–5.27 mm as well as dragging and holding the 185 gram body mass of the robot (Figure 2e). Joule heating was used with resistors while cooling was accelerated with an onboard fan between 25 °C and 65–70 °C. McEvoy et al. showed passive bending of a robot arm with low-melting point (60 °C) polycaprolactone (PCL, $T_g = -60$ °C) [53]. PCL was heated by Nichrome wires wrapped outside and encapsulated by silicone rubber. Yuen et al. used polylactic acid (PLA, $T_g = 65$ °C) or Acrylonitrile-Butadiene-Styrene (ABS, $T_g = 105$ °C) cables to enable long-time lifting of a robot arm without maintenance energy [54]. Encapsulated by polystyrene-block-poly(ethylene-r-an-butylene)-block-polystyrene (SEBS), the cables were heated with NiTi wires in the core and actuated by SMA in the outer layer for bending.

In particular, a subset of thermoplastics, i.e. thermoplastic SMP [25,55], has raised particular interest for variable rigidity in robot applications. SMP exhibits a significant reduction in elastic modulus when the temperature exceeds its T_g (Figure 2b). Elastic modulus of SMPs within the glass transition region is approximated as [56]:

$$G = G_g^{\left[a\left(\frac{T_g}{T}-1\right)\right]} \tag{1}$$

where G is shear modulus of the SMP at temperature T, G_g is the shear modulus of SMP at glass transition temperature T_g, a is a constant and

is material dependent. In regions away from glass transition regions, elastic modulus of the polymers can be predicted as [57]:

$$G = CT + D \tag{2}$$

where C and D are both constants.

Takashima et al. designed a bending actuator that is a pneumatic artificial muscle (PAM) with one side containing a SMP sheet with embedded Nichrome wires [26]. Upon heating, large bending curvature could be achieved and that curvature can be maintained afterward without additional energy. The SMP had a modulus of 1350 MPa under the 45 °C glass transition temperature and 4.5 MPa above the temperature. Yang et al. used a similar SMP for joints with variable stiffness in a three-joint nine-DOF arm [27]. The SMP had a modulus of 2150 MPa below the 45 °C glass transition temperature and 10 MPa above T_g. The main novelty of this work was that SMP was 3D printed on the joints by using the Fused Deposition Modelling technique (Figure 2d). Firouzeh et al. designed a tri-mode actuator which was composed of an air chamber and two variable stiffness side layers made by SMP [58]. By controlling the temperature of the two layers with embedded resistors, the actuator can bend in two contrary directions or elongate when compressed air flows in. The modulus of the SMP was 323 kPa and 560 kPa for the hot and cold binary states, respectively.

The magnitude of the tunable range for modulus may be increased by incorporating structural elements into the thermo-
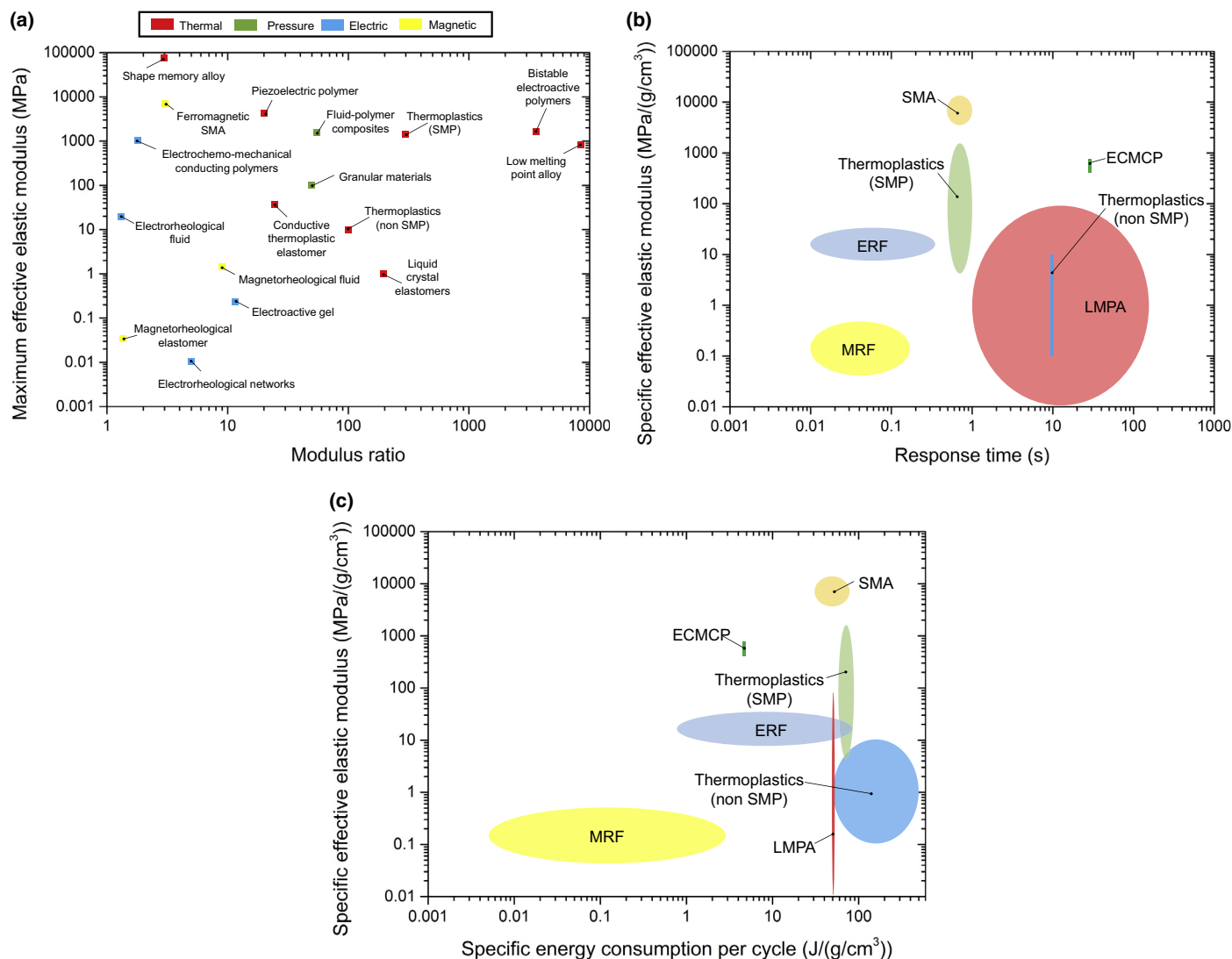
RESEARCH: Review

FIGURE 1

Quantitative analysis of variable rigidity materials. (a) Relation between maximal effective elastic modulus and modulus variation ratio, which is the ratio between the maximal and the minimal of effective elastic modulus. (b) Relation between specific effective elastic modulus (normalized by material density) and response time. (c) Relation between specific effective elastic modulus and specific energy consumption per cycle (normalized by material density).

plastics. Capadona et al. embedded carbon nanowhiskers into a PVAc matrix to create a rigidity-tuning nanocomposite capable of a three-order reduction in tensile storage modulus when temperature is increased from 25 to 55 °C [10]. McKnight et al. showed that the range of modulus variation can be increased to 0.17 ∼ 12.1 GPa by adding steel platelets to thermoplastic SMP [59]. Chen et al. found a similar result with the modulus variation range increased to 0.03 ∼ 2.7 GPa by adding steel tubes to thermosetting SMP [60]. The robot applications for these composites are yet to be demonstrated.

Besides thermoplastics, LMPAs have also been used for rigidity tuning. Nakai et al. used a type of LMPA in appendages for a robot hand and a quadruped robot [16]. The LMPA was heated by electro conductive fabric and encapsulated in silicone rubber. The LMPA has a melting temperature of 46.7 °C, and it took 3 min to heat it from 25 °C to 50 °C with 8 W and 5 min to cool it back passively in the air. The quadruped could climb up a lad-

der by bending legs to hold onto the ladder and prevent itself from falling [Figure 2h]. Cheng et al. used a combination of a LMPA and solder in both prismatic and bending joints for a mobile robot [61]. The combined alloy has a melting temperature of 70 °C and it was sandwiched between two strips of copper and heated by strain gauges from outside the copper. Shan et al. fabricated a tunable rigidity composite that could be used for robot mechanical structures [29]. The composite had a layer of a LMPA (melting point 62 °C) and another layer of gallium–indium–tin (Galinstan) alloy, which functioned as a Joule heating element. Both layers where embedded in a soft polyacrylate elastomer (3M VHB tape). The modulus of the LMPA could be varied between 0.86 GPa and 95.2 kPa between the room temperature and the melting temperature, and heating took 130 s with 3.6 W power. Schubert & Floreano fabricated a composite with a LMPA embedded in poly(dimethylsiloxane) (PDMS) [28]. The LMPA has a melting temperature of 47 °C and was directly
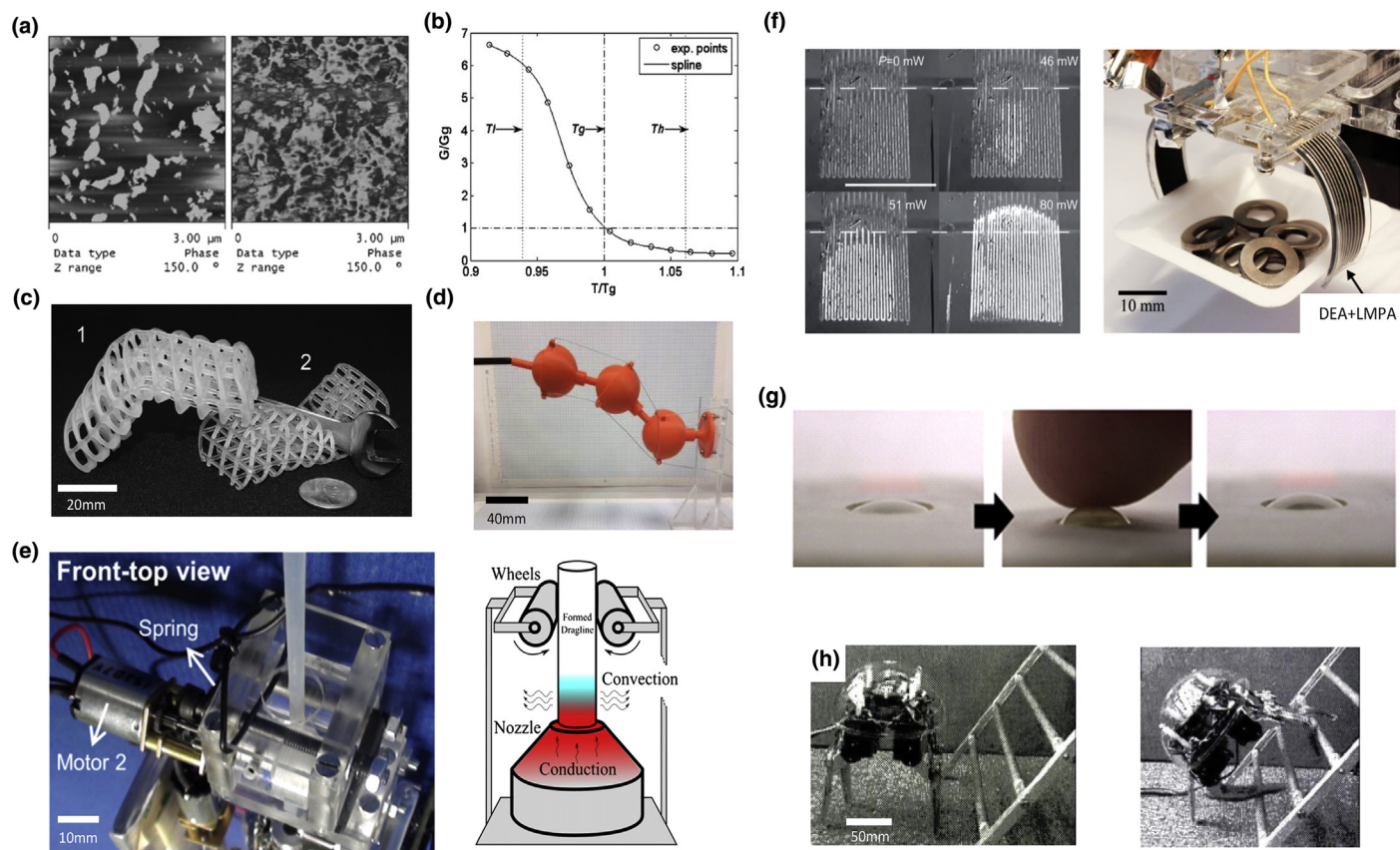
FIGURE 2

Thermally induced tuning of material rigidity. (a) Atomic force microscopy (AFM) phase images of thermoplastics PCL-PIBMD50. bright area = stiff phase, switching domains, and dark area = smooth phase, hard domains. Left panel: $T < T_g$. Right panel: $T > T_g$, switching domains are amorphous [52]. (b) Change of SMP's elastic modulus with temperature [105]. (c) A tunable stiffness structure by phase change of wax. (1) 3D-printed flexible scaffolds coated with wax, (2) uncoated with wax [64]. (d) A 3D printed hyper-redundant robotic arm utilizing the modulus tuning of SMP to realize variable stiffness. The robotic arm is cascaded by ball joints and actuated by cables [27]. (e) A dragline-forming mobile robot by tuning rigidity of thermoplastic adhesives [12]. (f) Variable stiffness device based on LMPA. Left: LMPA tracks encapsulated in PDMS with images when power is increasing. White areas indicate the melting portion of LMPA. Right: application in a variable stiffness gripper [15,28]. (g) Bistable electroactive polymers with tunable rigidity. (h) A metamorphic leg robot made of LMPA. The robot changes its leg shape during climbing a ladder [16].

heated with electrical power. With a power of 500 mW, the modulus of the composite could be reduced from 40 MPa at room temperature to 1.5 MPa at 50 °C in less than a second (Figure 2f).

More recently, Van Meerbeek et al. created a novel LMPA-elastomer composite with random porosity [62]. A porous elastomer foam is produced using an approach similar to that by Liang et al. for a creating liquid metal-filled PDMS sponge [63]. Next, it is filled with melted Field's metal using vacuum pressure. Lastly, the alloy is allowed to cool to room temperature and solidify. As with other LMPA-elastomer systems, the foam exhibits rigidity tuning, shape memory, and self-healing properties. The composite shows a rigidity change of 18× in tension and 30× in compression. By deforming the foam and freezing the LMPA, Van Meerbeek et al. could create elongated and twisted shapes. The natural (stress-free) shape of the composite is restored by raising the temperature and melting the LMPA.

In all, thermally-induced rigidity tuning can be electrically controlled with embedded and externally attached heating elements or materials in thermoplastics and LMPAs. A variation of up to 8600 times in modulus can be achieved with modulus

being as small as 0.1 MPa and as large as several GPa. Joule heating was mostly used and it can take a second to several minutes from room temperature to 60–70 °C with an electrical power under 10 W, while cooling is generally much slower when done naturally in the air.

Pressure induced

Pressure-induced rigidity tuning occurs in granular materials and fluid-polymer composites. Particle jamming has attracted interest due to the ability to rapidly transition between fluid and solid-like properties through small changes in granular volume fraction. Such transitions can lead to effective changes in material viscosity and rigidity. From optical micrographs, carbon black undergoes phase transition from fluid to solid state when volume fraction increases (Figure 3a, left panel) [65]. As a result, the phase change for granular materials leads to the variation of macroscopic properties, such as increase in viscosity at liquid state and increase in elastic modulus at solid state as volume fraction increases (Figure 3a, right panel).

When the jamming system is in liquid state, the viscosity η is calculated as [65]
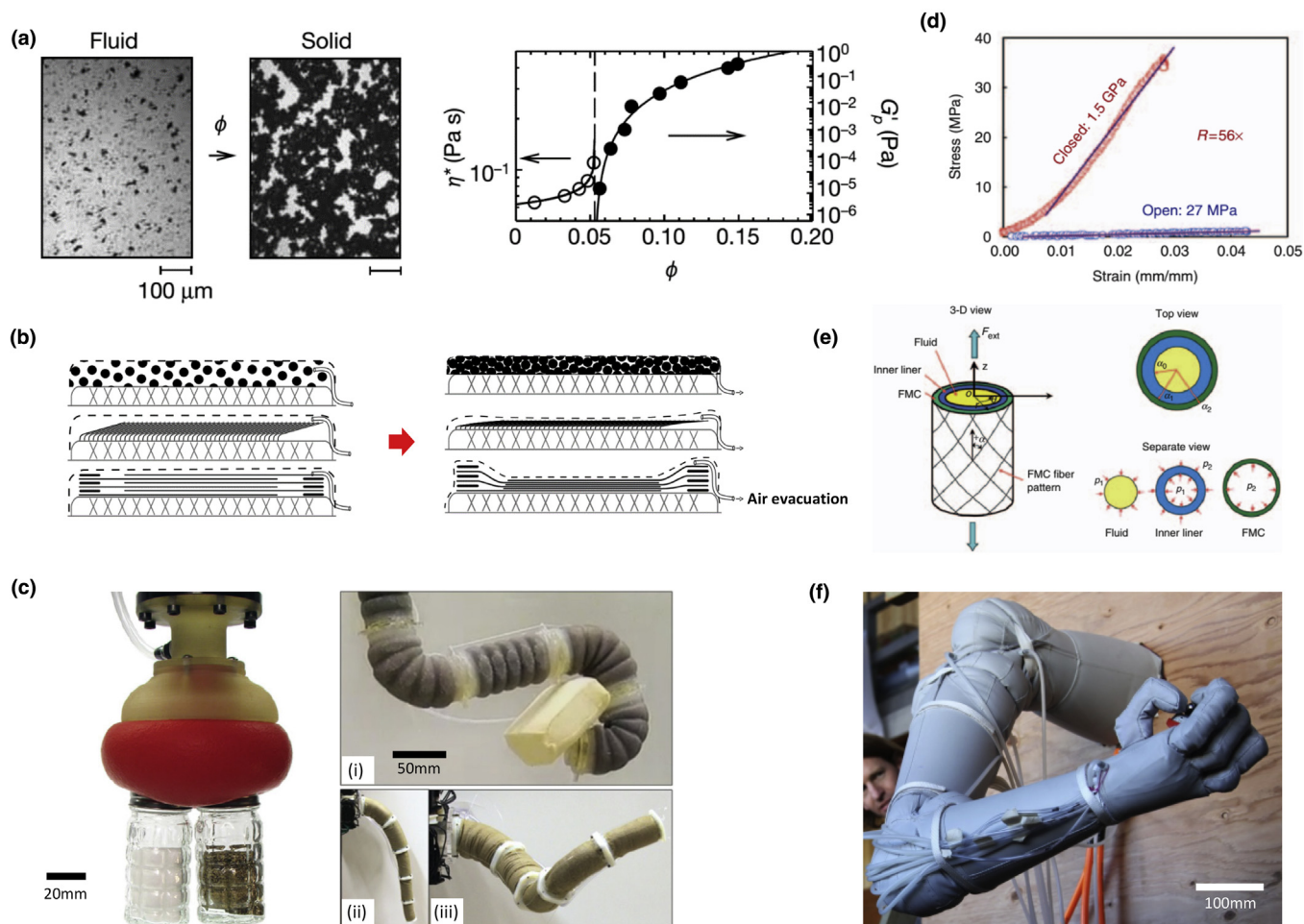
FIGURE 3

Pressure-induced tuning of material rigidity. (a) Phase transition for carbon black. Left panel: optical micrographs presenting the transition from fluid state to solid state. Right panel: the volume fraction Φ's increase lead to increase in viscosity η and elastic modulus G'p [65]. (b) Working principle of three jamming compartments on top of pneumatic actuators including granular jamming, layer jamming with overlapping fish-scale-like layers and layer jamming with two stacks of three interleaved layers. Left panel: unjammed state. Right panel: jammed state with air evacuation [70]. (c) Granular jamming robotic applications. Left panel: A universal gripper grasping multiple objects at once with air evacuation [36]. Right panel: an articulated manipulator with integrated granular materials. (i) Grasping an object; (ii) manipulator in unjammed state; (iii) manipulator jammed in a corkscrew configuration [66]. (d) Stress–strain curve of a fluidic flexible matrix composite tube composed of ±35° carbon fiber/silicone matrix [19]. (e) Illustration of the fluidic flexible matrix composite tube. (f) An inflatable manipulator prototype [73].

$$\eta = \eta_s(\phi_c - \phi)^{-\gamma_\phi}. \tag{3}$$

The effective shear modulus G'_p in the solid state is approximated as

$$G'_p = G'_\phi(\phi - \phi_c)^{\nu_\phi}, \tag{4}$$

where ϕ is the particle volume fraction, $\gamma_\phi \approx 0.13$ and $\nu_\phi \approx 4.0$, η_s is the solvent viscosity; both G'_ϕ and ϕ_c depend on the interparticle attractive energy, U. In robotics applications, the particle volume fraction is controlled by internal air pressure [36], which allows for a direct mapping between pressure and effective measures of viscosity and shear modulus.

The phase change of granular matter has been widely adopted for robotic applications where rigidity tuning is needed. One example is the universal gripper reported in [36], which exhibits good adaptability and conformability when grasping objects of different shapes and sizes (Figure 3c, left panel). Another application of particle jamming is the articulated cable-driven

manipulator reported by [66]. In this implementation, granular matter enables reversible transitions between a flexible, hyper-redundant state and a rigid state capable of supporting large payloads (Figure 3c, right panel). In both applications, stiffening requires air to evacuate from the granular medium. For the positive pressure universal gripper proposed by Amend et al. positive and negative pressure were combined to modulate the jamming transition of the gripper [36]. Positive pressure was applied to make the transition faster and more reversible, as well as adding capability to shoot objects by fast ejection. Cheng et al. also investigated prosthetic jamming terminal devices to help the disabled [67]. It was an attempt to apply research to real-world applications. The main roadblock they found was the lack of small, lightweight and quiet pneumatic power that could be operated rapidly, and most importantly, commercially available.

Aside from gripping and manipulation, pneumatic jamming has also been used for soft robot locomotion. Steltz et al.

proposed a rolling robot enabled by selectively jammed cells filled with granular materials [34]. They investigated the flexural rigidity of different material combinations, and found that the effective flexural modulus of a thin flexible plastic cylindrical beam filled with salts increased from 0 to 5 MPa when vacuum level varied from 0 to −74.5 kPa (0 stands for atmospheric pressure). For the rolling robotic design, fluidic actuator was wrapped inside a number of cells. Controlling the rigidity of different cells with jamming, the robot was enabled with shape changing ability as well as rolling locomotion. Wei et al. integrated soft pneumatic actuators with packed granular materials for soft grippers possessing both variable stiffness and shape adaptation to irregularly shaped objects [68]. Stiffness tests performed with the soft finger revealed that the finger stiffness in the lateral bending plane was 0.018 N/mm at 0 vacuum pressure and increased to 0.186 N/mm at −90 kPa vacuum pressure. The stiffness range was more than 10× for one finger. Grasping demonstrations were also performed by installing the developed grippers on a dual-arm robot. Granular materials for rigidity tuning have also been applied in surgical robots for MIS. A modular surgical manipulator proposed by Cianchetti et al. composed of three fluidic chambers equally spaced in a radial arrangement and the central channel filled with granular materials for rigidity tuning. The manipulator exhibited 46% stiffness increase when the central channel filled with coffee powder was vacuumed from 0 to −91 kPa [69].

Planar pneumatic jamming with a layered architecture has also been investigated and rigidity enhancement was observed during air evacuation (Figure 3b) [70]. The confined vacuum pressure increases the friction between overlapping layers and thus contributes to an effective increase in flexural rigidity. Kim et al. proposed a tubular snake-like manipulator for minimally invasive surgery (MIS) based on layer jamming [71]. The manipulator exhibited 3.8 N resisting force at vacuum level −101 kPa and 2 N at −33.3 kPa when displacement at the manipulator's tip was 20 mm. Compared with other MIS prototypes, the proposed layer jamming manipulator possessed relatively long length and small diameter, while maintaining the ability for high payload, which was promising for MIS applications.

Another category of materials whose rigidity may be varied by pressure include fluid–polymer composites. Due to the variable bulk modulus of fluids, the effective modulus of the composites can be varied by pressure. Shan et al. proposed a fluidic flexible matrix composite (FMC) composed of carbon fiber tubes and a silicone matrix [19]. The tubes use a polyacrylonitrile-based carbon fiber and have an outside diameter of 13.5 mm (Figure 3e). By modulating the internal air pressure, the composite exhibited a 56× change in modulus, which ranged between 1.5 GPa and 27 MPa (Figure 3d). In a similar phenomenon at the macroscopic level, an air beam made of rubber or plastic fabrics is filled, so that the inflated air beam can be stiff enough to bear loads. This phenomenon has been widely used to construct lightweight robot arms [72–75] (Figure 3f).

Rigidity variation for pressure induced granular materials can be achieved around 1.1 s for stiffening while 0.1 s for loosening [36]. The effective modulus range can be 50 times, from 2 MPa to 100 MPa when vacuum level changes from −1 kPa to −80 kPa [35]. One drawback of pressure-induced materials is that the hardware required for providing pneumatic power are currently large, noisy and heavy, making them unsuitable for compact or portable operations.

Magnetic field induced

Magnetic field induced rigidity tuning has been found in MR fluids, elastomers, and networks that can be stimulated under applied magnetic field. As seen in SEM micrographs, iron spheres of 1–3 μm (Figure 4a, left panel) and iron microwires of 7.6 μm (Figure 4a, right panel) in MR fluids form chains in the direction of magnetic field [76]. This change at the microscopic scale leads to viscosity change at the meso/macroscopic scale. MR elastomers are produced by distributing the iron particles into elastomers, which results in magnetically tunable elastic modulus (Figure 4b) [40]. Specifically, the elastic modulus of the MR elastomers increases by increasing applied magnetic flux density. The elastic modulus increases significantly starting from 30 mT while it tends to level off from 200 mT. Additionally, increasing the concentration of iron particles would increase the elastic modulus of the composite, accordingly.

The shear modulus of MR fluids is also observed to vary under applied magnetic field. The rigidity change of MR fluids can be represented by a change in shear modulus, G, which is approximated as [77]:

$$G = \sqrt{6}\phi\mu_0 M_s^{\frac{1}{2}}H^{\frac{3}{2}}, \tag{5}$$

where ϕ represents the particle concentration, μ_0 is the permeability of free space, M_s is the saturation magnetization of the magnetizable particles, and H is the strength of applied magnetic field. Modeling of MR elastomers was conducted by Davis using structural finite element analysis [78]. In his study, the shear modulus response of MR elastomers induced by magnetic field was theoretically predicted.

The liquid state of MR fluids is suitable for application domains where delicate manipulation and passive adaptation are required, such as food handling in the agricultural and service industries. A robotic gripper based on MR fluids is able to realize passive shape conformation when grasping objects with different geometrical shapes (Figure 4c) [79]. During grasping, magnetic field is not applied and the MR fluids encapsulated in the gripper can easily flow and conform to objects with large surface contact. When magnetic field is applied, the rheological property of MR fluids is changed and the increased viscosity contributes to high stiffness of the gripper, making the grasped object ready for transportation. From a grip strength test, grip strength for tomatoes with magnets activated is around 9 N and only 4 N when inactivated at a grip gap of 3 mm.

MR fluids can be used for exoskeletons prosthetic knees to realize adaptive control of torque [80,81]. Herr et al. found that MR brakes in prosthetic knees could produce a torque ranging from 0.5 Nm to 40 Nm by controlling the magnetic field intensity. MR fluids have also been adopted in haptic devices. For example, haptic joysticks perform quite differently for wall collision with and without the spherical MR-brakes [39].

MR elastomers (MRE) have also gained robotic applications such as in prosthetic devices. Thorsteinsson et al. proposed a prosthetic device with an MRE spring placed on the vertical axis to provide alterable stiffness dynamically [21] (Figure 4d). In their design, the stiffness of shock absorption member is
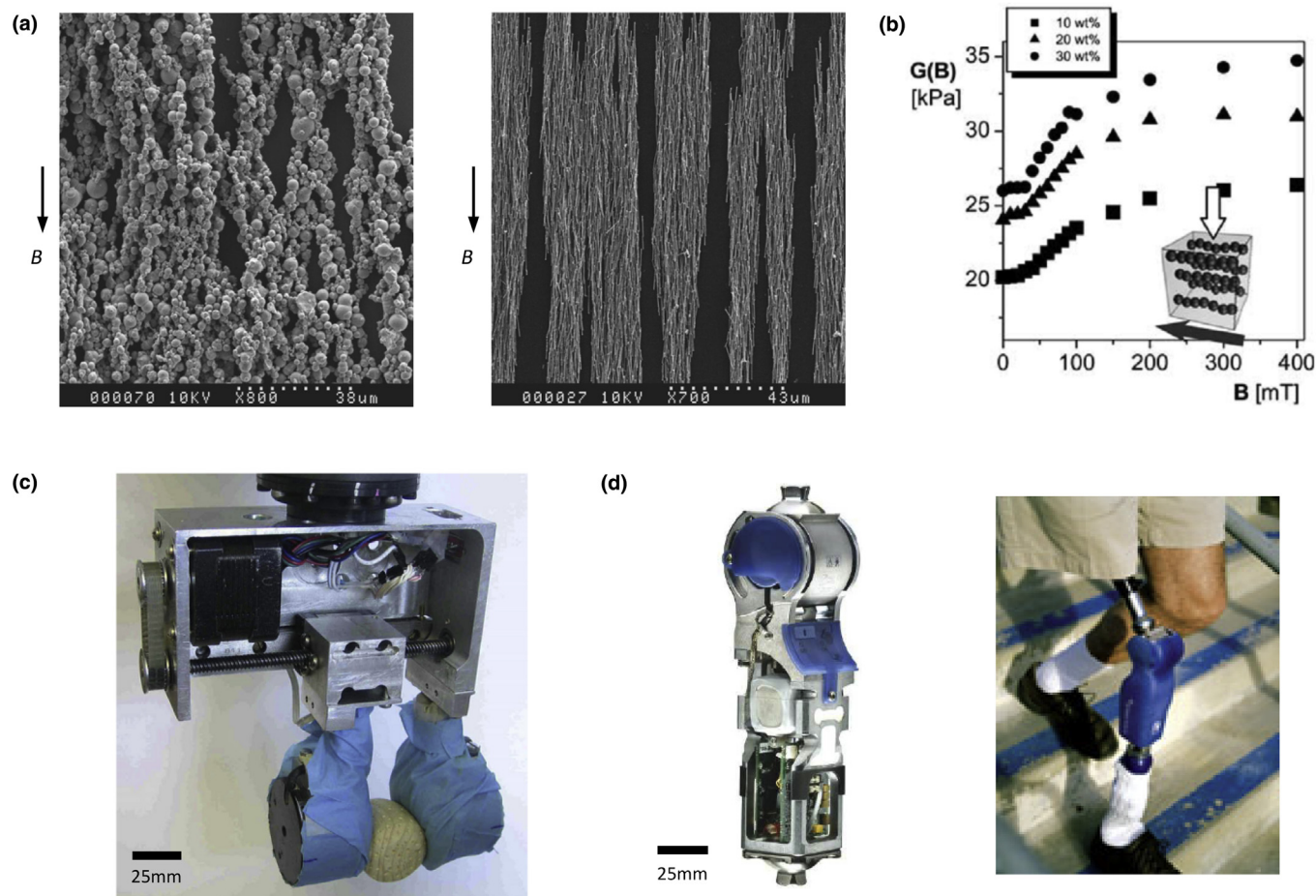
FIGURE 4

Magnetic field-induced tuning of material rigidity. (a) SEM micrographs of MR fluids. Left panel: 1–3 μm iron spheres in the presence of a planar 0.26 T magnetic field. Right panel: 7.6 μm iron microwires in the presence of a planar 0.26 T magnetic field [76]. (b) MR elastomers with tunable elastic modulus. The figure shows effect of the magnetic field intensity on the elastic modulus. The white and black arrows indicate the direction of the force and the uniform magnetic field respectively [40]. (c) A robotic gripper realizing passive shape conformation by changing rheological properties of MR fluids [79]. (d) A commercial prosthetic device with an MRE spring placed on the vertical axis to provide alterable stiffness dynamically [21].

140 N/mm at low activity levels and 178 N/mm at high activity levels.

MR materials can be activated in a fraction of a millisecond [38] and in 170 ms for a MR fluid-based haptic device [39]. The tensile modulus of an elastomer embedded with overlapping plastic surfaces separated by MR fluid can vary by a factor of nine, from 0.1644 MPa to 1.4658 MPa, when applied magnetic field is increased from 0 to 35 mT [82]. Compared to thermal induced and pressure induced materials, which realize rigidity tuning isotropically, magnetic field induced materials show anisotropy during rigidity tuning. Rigidity range is larger in the direction perpendicular to the direction of iron particle chains. Affiliated equipment, such as electromagnets, to produce the magnetic stimulus are essential, but have yet to be solved, for these materials to be applied in compact and low weight robotic systems. Previously, MR materials have been widely used in brakes and dampers with only limited applications in robotic fields. The rapid progress of soft robotics will broaden the application of these materials in situations where more adaptive robotic bodies, hands, or legs are needed.

Electric field induced

Electric field-induced rigidity-tuning methods primarily include ER fluids (ERF), ER elastomers, or electrorheological networks (ERNs). The latter are composed of semiconducting particles embedded in polymer matrices exhibiting tunable elastic modulus under the application of electric field. Chin et al. observed the microstructures of cross-linked ERN containing 2 wt.% colloidal particles of semiconducting polyaniline under applied electric field [42]. As the pre-alignment electric field strength E_0 increases, the dispersed particles become aggregated to form chains along the electric field's direction (Figure 5a, left panel). The shear modulus of ERN increases with the increase in operating electric field's strength. For an ERN with $E_0 = 1000$ V/mm and with 20 wt.% semiconducting polyaniline particles, the shear modulus ranges from 2 kPa to 10 kPa when applied electric field increases from 1000 V/mm to 3000 V/mm (Figure 5a, right panel). The difference of slope for different pre-aligning electric fields is attributed to the complicated electrical properties of the ERNs.
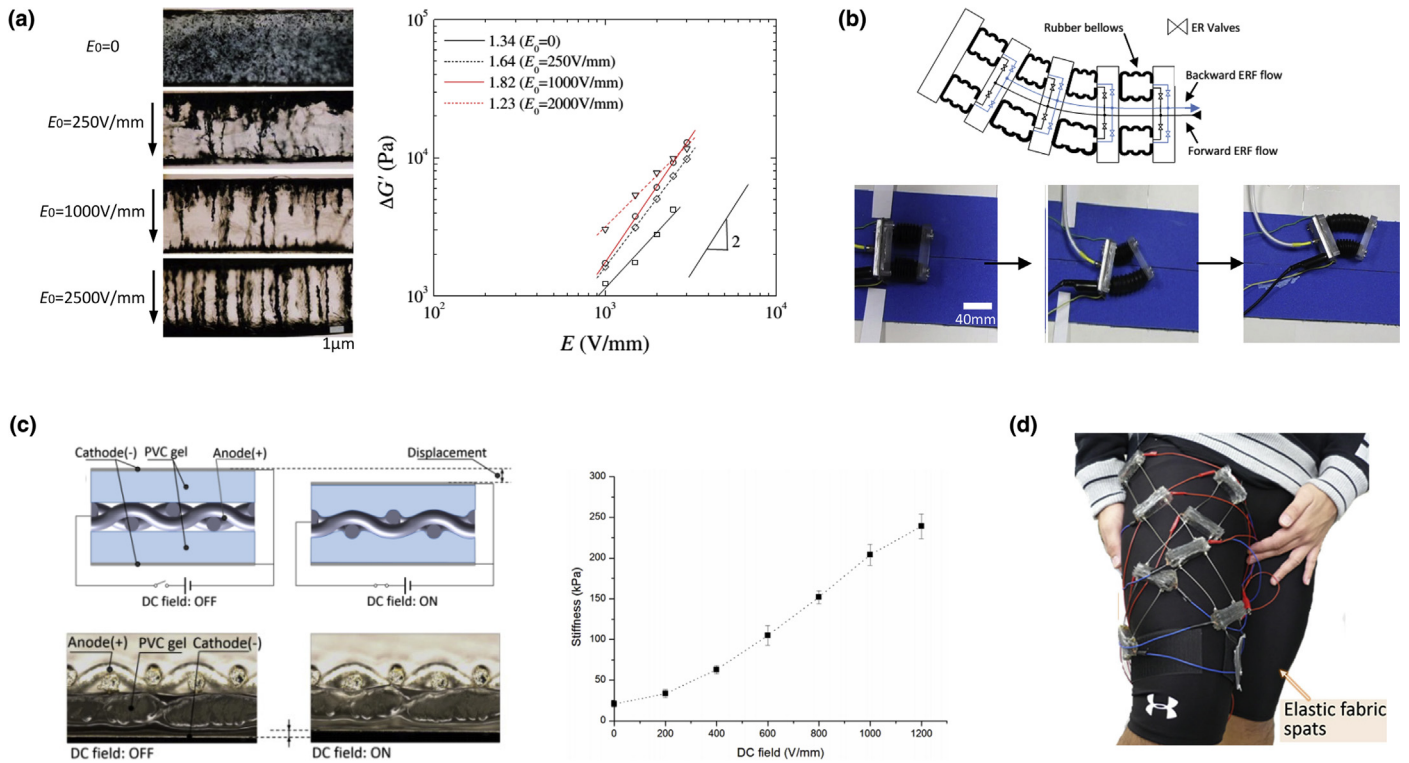
FIGURE 5

Electric field induced tuning of material rigidity. (a) Electrorheological network (ERN) with semiconducting particles embedded and partially aligned to form particle strings or columns. Left panel: microstructures of cross-linked ERN (cross section view). Right panel: ERN's shear modulus variation with operating electric field strength. The pre-aligning electric field strength was varied as $E_0 = 0$ (*open square*), 250 V/mm (*open diamond*), 1000 V/mm (*open circle*), and 2000 V/mm (*open inverted triangle*) [42]. (b) A robot based on ERF valves controlling the forward/backward ERF flow, which can move forward by the elongation and retraction of bellows [85]. (c) Mechanism of PVC gel actuator. Left upper panel: mechanism diagram. Left bottom panel: experimental result. Right panel: modulus variation with electric field in a 15-layer PVC gel [23]. (d) A wearable device with eight PVC gel actuators with variable stiffness which functions similar to that of biological muscles [23].

For ER fluids based on pine oils, the total viscosity η can be calculated by [83]:

$$\eta = \eta_0 M_n^{-d} \tag{6}$$

where η_0 is the absolute viscosity, d is the shear-thinning exponent. The shear-thinning exponent increases when the electric field strength increases and usually for ER fluids $0.68 < d < 0.91$. M_n is the Mason number, which indicates the relation between viscous force and polarization force and can be calculated by:

$$M_n = \frac{24\pi\eta_a\dot{\gamma}}{(\beta E)^2} \tag{7}$$

where η_a is the apparent viscosity of the rheological fluid at the application of the electric field, γ is the shear strain rate, $\beta = (K_p - K_f)/(K_p + 2K_f)$ is the dielectric mismatch parameter, K_p the relative permittivity of the particle, K_f is the relative permittivity of the carrier liquid, and E is the electric field.

Nikitczuk et al. developed a portable active knee rehabilitation device based on the integration of an ERF brake into a knee orthoses [84]. The resistive torque of the device ranges from 20 Nm to 120 Nm when applied fields varied from 0 to 4000 V/mm. Close-loop control of torque and velocity was realized and tested in the proposed device, prospected for accelerating motor recovery in knee injury or stroke patients. The tunable rheological property of ERF was also used for the valve design by Sadeghi et al. and the flow of ERF was controlled by applied voltage [85]. In their further investigation, the flow rate of ERF in the cylindrical valve with valve gap of 1 mm dropped from 780 mm^3/s to 0 when applied electric field increased from 0 to 3000 V/mm (inlet pressure is 0.07 MPa) [43]. Utilizing this valve in a soft fluidic continuum arm, the robot is able to crawl by controlling the forward/backward flow of ERF (Figure 5b). Using ER micro valves, Yoshida et al. also developed a micro gripper based on micro-electro-mechanical systems (MEMS)-based architectures [86]. In addition to ERF brakes and valves applied in robotics, Kenaley et al. investigated ER fluids integrated into robotic fingertips for tactile sensing [87]. In their design, ER fluids sandwiched between elastomer and positive electrode formed a capacitor capable of sensing applied force due to the elastomers' deflection. The ER fluids could also change from Newtonian fluid to Bingham plastics when energized for better shape adaption and inner-locking when grasping.

One advantage of ER-based robotics over MR materials is that ER materials are more compatible in magnetic resonance imaging (MRI) environments. However, it is worth noting that ER fluids are normally operated at a relatively high voltage 1–5 kV [43]. The high voltage is not a preferred factor when applied on service robotics, where safety is of primary concern, or portable robotics, where equipment to produce high voltage is cumbersome. Therefore, the future challenge is to solve these issues for better application of electric field-induced materials in robotics.

Besides ER fluids and ER networks, electroactive gel can also exhibit variable rigidity with electrical fields. This was first found in echinoderms, which have a dermis that becomes stiff when the cells are lysed. The result was caused by the purification of a protein acting as stiffener to make the dermis stiffen [88]. Li et al. showed a 15-layer polyvinylchloride (PVC) gel that exhibited a modulus change from 20 kPa at 0 V/mm to 240 kPa at 1200 V/mm (Figure 5c) [23]. A wearable device was then fabricated and tested on human subjects (Figure 5d).

Other potential materials

In addition to the aforementioned materials, whose variable rigidity has been proven for robot applications, other potential materials exist to be explored in future research.

Shape memory alloys (SMAs) have been used as actuators in robotics [31] and beyond [32]. Besides the shape memory effect, SMAs also exhibit variable rigidity, which may be induced thermally through direct electrical Joule heating. Mavroidis showed that NiTi, a type of thermal SMA, has modulus of 28–41 GPa as a Martensite and 83 GPa as an Austenite [30]. Besides thermal induction, modulus of some SMAs can also be varied by magnetic field or mechanical loading. Faidley et al. found a modulus defect in $Ni_{50}Mn_{28.7}Ga_{21.3}$, whereby the elastic modulus increases as much as 255% upon increasing the applied magnetic field from zero to 380 kA/m DC [89]. Couch et al. determined Young's modulus of NiMnGa in its field and stress preferred configurations to be 450 MPa and 820 MPa respectively across 5.8% strain [50]. The actual benefit of variable rigidity in SMA to robot and other applications is yet to be found [2]. For example, thermoplastic encapsulating an SMA was used as multi-functional fiber [54]. The fiber can be applied as artificial muscle when actuation is needed, and as a variable stiffness functional part when different stiffness is needed.

EAPs other than ER fluids and ionic gel may also be used in a rigidity-tuning component. For example, liquid crystal elastomers' modulus can be varied between 1 MPa at room temperature and approximately 5 kPa at 80 °C [33,90]. They may also be tuned by mechanical strain [91–93]. Electrochemo-mechanical conducting polymers [47] have also shown possibilities of variable modulus. Thermochemo-mechanical elastomers [94] comprising Diels-Alder cycloaddition reaction moieties could be switched between different crosslinking density states and thus exhibited variable modulus. The elastomer exhibited 3 times modulus change from 0.4 MPa to 1.2 MPa. Electrically induced actuation strain up to ~50% was obtained at both rigid and soft states with energy density in the same range as muscle. For dielectric elastomers, no evidence for variable modulus has been found, however it was shown that a 20-mm strip had 21% reduction in average stiffness from 92 N/m to 73 N/m upon the application of 4-kV electric voltage [1], but this could be due to the geometric change of the strip.

Thermoplastic elastomer (TPE) copolymers may have variable rigidity induced thermally. Shan et al. added carbon black into a TPE, which were then encapsulated in PDMS [17]. By supplying electrical power, the conductive TPE (cTPE) can heat itself and soften. Tensile modulus for the PDMS composite could be varied between 37 MPa at room temperature and 1.5 MPa at a temperature above 75 °C. The heating response time was six seconds with 0.17–3.3 W power. The response time is improved by coating the cTPE film with liquid metal electrodes composed of eutectic gallium indium [95]. When coated on its surfaces, electrical current travels through the thickness of the film and allows for softening response in under 1 s when 20 V bias is applied. Applications that have been explored include shape conformable splints [95] and tendons with tunable load-bearing properties [96].

Wax is another type of material whose rigidity may be tuned by temperature change [97]. Cheng et al. used wax to coat polyurethane which varied elastic modulus between 200 kPa at 25 °C and 10 kPa at 70 °C due to wax coating [64]. The combination was made into foam and lattice structures (Figure 2c) to demonstrate the ability to form ordered structures in robotic systems. Heating was done with copper wires wrapped around the structures.

Bistable electroactive polymers (BSEP) behave like typical SMP with regard to modulus change with temperature [51]. The main difference is that the BSEP could be electrically actuated to large strains at the softened state to realize various shapes, reversibly. The first BSEP based on a thermoplastic polymer [51] exhibited actuation strains as large as 300%, but with a rather large transition temperature range typical of an SMP. When phase-changing moieties were incorporated to obtain large modulus change via reversible melting of nanocrystalline phases, the transition temperature range was narrowed to within 5 °C [98]. Further, the transition temperature could be tuned to around human body temperature, which could be desirable in designing robotic application gears for individual persons. The actuation cycle of BSEP is shown in Figure 2g.

Piezoelectric polymers have also shown the possibility of rigidity variation. Date et al. found that the storage modulus of poly(y-methyl L-glutamate) varied from 1–4 GPa to 0.2–2 GPa at 100 °C [48]. Although suggested by Shan et al. [19], there remains to be direct evidence of tunable rigidity in piezoelectric ceramics and magnetostrictive ceramics. In any case, ceramics have not been widely used in robotics other than as microactuators due to their brittleness.

Discussion and outlook

For quantitative assessment of rigidity-tuning materials, four measures are found to be particularly useful. First, the magnitude of specific effective elastic modulus determines the stiffness of a structure and the force and deformation that a robot can generate or withstand. Second, the ratio between the maximal and the minimal rigidity influences the choice of actuators in a robot. Third, response time of variation directly determines the dynamic tasks the robot is suitable for. Last, energy consumption required for state transitions determines the choice of energy sources for the robot. We collected data on these measures for all the materials from literature (Table 2) and identified the correlation between them (so long as data was available). It is worth noting that the best effort was made to select data from the same study that reported the largest ratio of modulus variation, the shortest response time, and the lowest power consumption. Otherwise data from the work with the largest ratio of modulus

TABLE 2

Quantitative comparison of rigidity tuning.

Material Type	Variation Range	Increase response time	Decrease response time	Power consumption	Density
Thermoplastics (non-SMP)	0.1–10 MPa ($>T_g$) [24]	120 s [24]	10 s [24]	5–50 W [24]	1 g/cm^3 [24]
Thermoplastic SMPs	0.1–10 MPa ($>T_g$) 0.01–3 GPa ($<T_g$) [25] 4.5 MPa ($>T_g$) 1350 MPa ($<T_g$) [26]	120 s [27]	0.5–1 s [26]	80–125 W [26]	0.9–1.1 g/cm^3 [25]
LMPAs	1.5–40 MPa [28] 0.0952–860 MPa [29]	10–60 s [28]	0.8–2.3 s [28] 130–140 s [29]	0.3–0.7 W [28] 3.6 W [29]	9.7 g/cm^3 (Field's metal) [29]
cTPE	1.5–37 MPa [17] 0.7–10.4 MPa [95]	N/A	6 s [17] 1 s [95]	0.17–3.3 W [17]	N/A
SMAs	28–83 GPa [30]	0.5–1 s [31,32]	0.3–14 s [32]	480 W [30]	6–8 g/cm^3 [30,32]
LC elastomers	0.005–1 MPa [33]	N/A	N/A	N/A	N/A
Granular materials	2–100 MPa [34,35]	1.1 s [36]	0.1 s [36]	21.25–1339.2 W [36]	Variable with volume fraction
Fluid-polymer composites	0.027–1.5 GPa [19]	~1 s [19]	N/A	N/A	N/A
MR fluids	0.1–1 Pas [37]	0.01–0.17 s [38,39]	N/A	2–50 W [37]	3–4 g/cm^3 [37]
MR elastomers	26–35 kPa [40]	<0.01 s [41]	N/A	N/A	N/A
ER networks	2–10 kPa [42]	N/A	N/A	N/A	N/A
ER fluids	0.078–0.16 Pas [43]	0.01–0.34 s [22,44]	N/A	150 W [45]	0.6–2 g/cm^3 [46]
ECMCPs	0.6–1.06 GPa [47]	30 s [47]	N/A	0.23 W [47]	1.452 g/cm^3 [47]
Electroactive gel	20–240 kPa [23]	N/A	N/A	N/A	N/A
Piezoelectric polymers	0.2–4 GPa [48]	N/A	N/A	N/A	N/A
Magnetic SMAs	2.4–7.3 GPa [49]	N/A	N/A	N/A	8.36 g/cm^3 [50]
Bistable EAP	0.42–1500 MPa [51]	N/A	N/A	N/A	~1 g/cm^3 [51]

variation were used due to the possible existence of trade-offs between these measures.

We relate the maximal value of the effective modulus to the ratio between the maximal and the minimal value (Figure 1a). We have found that LMPAs have the largest modulus variation ratio (8600 times) and a large maximal modulus (860 MPa). SMPs are also efficient at both, with a ratio of 300 times and a maximal modulus of 1350 MPa. MR elastomers have both the smallest maximal modulus of 35 kPa and the smallest modulus ratio of 1.35 times. Other materials with small ratios include SMAs, magnetic SMAs, ECMCPs, and elastomer-encapsulated ER fluids. From the perspective of induction method, electric- and magnetic-induced materials exhibit small modulus ratios, ranging from 2 to 10 (Figure 1a). As for pressure-induced materials, it is interesting that fluid-polymer composites and granular materials have very close modulus ratio, both from 50 to 60. Thermal induction covers a large category of materials and the modulus ratios are generally over 100. We have also noticed all the listed variable rigidity materials cover the top left part of the design space, meaning a material with a large modulus variation ratio and a small maximal modulus is not available.

Next, we relate the specific effective modulus to the response time of induction (Figure 1b). Here, specific effective elastic modulus is defined as the effective elastic modulus normalized by the density of the materials to remove the effect of size and mass [99]. It has practical meaning, as a higher value enables lightweight structures given the same structural stiffness. Since there are two response times related to both increase and decrease in rigidity, we use the response time associated with energy

consumption in the relevant induction method. Although it is obvious that rigidity-tuning materials that require thermal activation have a longer response time than those with other stimulation methods, it is interesting to see that the response time varies largely among thermally induced materials. For example, the response time was 130 s for LMPAs [29] and less than 1 s for non-SMP thermoplastics like conductive propylene-based elastomer composites [95]. Another phenomenon is materials with a larger specific effective elastic modulus tend to need a longer response time. For example, ECMCPs have a specific effective modulus of 730 MPa/(g/cm^3) and need 30 s to increase modulus with electric induction.

We finally relate the specific effective modulus to the specific energy consumption in a single cycle of rigidity variation (Figure 1c). A strong correlation is found with the magnitude of the specific effective elastic modulus. For example, the specific effective elastic modulus of SMAs is five orders of magnitude higher than that of MR fluids, and needs three orders of magnitude more energy to vary rigidity.

It would be ideal to have materials that attribute all the characteristics listed above. However, after two decades of development, it is still not possible to achieve a combination of large rigidity variation, a fast response, and energy efficient tuning [1]. Overall, SMPs, non-SMP thermoplastics, LMPAs, TPEs, granular materials, fluid-polymer composites, MREs, MRFs, ERFs, and electroactive gels have been used for rigidity tuning in robot applications. As shown in Table 1, all these materials are semi-active, and no active rigid-tuning materials have been demonstrated applications in robotics. Specifically, SMPs seem to have a great potential, if energy efficiency is further improved, or

energy consumption is not a concern. This may explain why SMPs have attracted much attention [2] and have been used in grasping and manipulation. However, SMPs are not conductive and hence cannot be directly powered through Joule heating, therefore, require embedded heating elements. Electrically conductive SMP composites are worth further investigation. While SMP composites exhibit larger maximal modulus than SMPs, the effects of the composite filler on modulus variation range and response time remain to be further studied. BSEPs, a combination of SMP and dielectric elastomer, offers interesting attributes thanks to the large modulus change and large electrically actuation strain. Like the SMPs, the thermal activation responds rather slowly, while the electrical actuation requires high driving voltages like dielectric elastomers. Other interesting materials include LMPAs, non-SMP thermoplastics and TPEs, which have been used in grasping and ladder climbing. However, more characterization is required for the application of thermally activated materials in robotics, such as LCEs. Pressurized materials may be useful because they offer significant modulus changes and fast response. Granular materials and fluid-polymer composites have been used in grasping, ground locomotion and load bearing. However they are reliant on pumps, valves, and other external pneumatic hardware. Although ERF, MRF, and MRE have been used in manipulation, ground crawling, prosthetic devices and haptic interfaces, they are not satisfactory variable-rigidity materials due to the small specific modulus of MR fluids and the small ratio of ER fluids.

Besides variation in rigidity, responses in other aspects or properties of materials to their corresponding induction methods are worth discussion. For thermal induction, strain and recoverable strain are temperature dependent in SMPs [101,102] and the effect of strain on electrical conductivity in certain SMP composites can be complicated [103]. For pressure induction, not only viscosity but also yield stress increases with particle volume fraction in granular materials [65]. A similar effect of particle volume fraction on yield stress is also found in MR fluids with magnetic field induction [37] and ER fluids with electrical field induction [104].

Several grand challenges exist to find the optimal design of variable rigidity materials for robot applications. First of all, factors that influence the rigidity range, tuning speed and tuning power need to be identified. Second, tradeoffs between these properties must be further explored for the different material classes. Third, for solids in a low-modulus state, or for fluids, it is likely that they are incapable of holding their weight, thus further studies of material encapsulation are required. Fourth, computer optimization techniques may be used to design microstructures in materials to achieve the optimal performance in variable rigidity [100]. Last, a deeper study of rigidity-tuning mechanisms in natural organisms, from a materials perspective, could lead to the development of novel approaches in robotics applications.

Funding

References

[1] R.D. Kornbluh et al., Rubber to rigid, clamped to undamped: Toward composite materials with wide-range controllable stiffness and damping, Proc. SPIE 5388 (2004) 372–386.

[2] I.K. Kuder et al., Variable stiffness material and structure concepts for morphing applications, Prog. Aerosp. Sci. 63 (2013) 33–55.

[3] M. Manti, V. Cacucciolo, M. Cianchetti, Stiffening in soft robotics: a review of the state of the art, IEEE Rob. Autom. Mag. 23 (3) (2016) 93–106.

[4] C. Majidi, Soft robotics: a perspective – current trends and prospects for the future, Soft Rob. 1 (2014) 5–14.

[5] D. Rus, M.T. Tolley, Design, fabrication and control of soft robots, Nature 521 (2015) 467–475.

[6] L. Wang, S. G. Nurzamann, F. Iida, Soft-Material Robotics, now Publishers, Boston & Delft, 2017.

[7] F. Ilievski et al., Soft robotics for chemists, Angew. Chem. Int. Ed. 50 (2011) 1890–1895.

[8] S. Bauer et al., A soft future: from robots and sensor skin to energy harvesters, Adv. Mater. 26 (2014) 149–162.

[9] L. Wang, F. Iida, Deformation in soft-matter robotics, IEEE Rob. Autom. Mag. 22 (3) (2015) 125–139.

[10] J.R. Capadona et al., Stimuli-responsive polymer nanocomposites inspired by the sea cucumber dermis, Science 319 (5868) (2008) 1370–1374.

[11] F. Iida, S.G. Nurzaman, Adaptation of sensor morphology: an integrative view of perception from biologically inspired robotics perspective, Interface Focus 6 (4) (2016) 20160016.

[12] L. Wang, U. Culha, F. Iida, A dragline-forming mobile robot inspired by spiders, Bioinspir. Biomim. 9 (2014) 016006.

[13] Y. Yang et al., Bioinspired robotic fingers based on pneumatic actuator and 3D printing of smart material, Soft Rob. 4 (2) (2017) 147–162.

[14] A. Firouzeh, M. Salerno, J. Paik, Stiffness control with shape memory polymer in underactuated robotic origamis, IEEE Trans. Rob. 33 (4) (2017) 765–777.

[15] J. Shintake, et al., Variable stiffness actuator for soft robotics using dielectric elastomer and low-melting-point alloy, in: IEEE/RSJ Int. Conf. Intelligent Robots and Systems, 2015, pp. 1097–1102.

[16] H. Nakai, et al., Metamorphic robot made of low melting point alloy, in: IEEE/RSJ Int. Conf. Intelligent Robots and Systems, 2002, pp. 2025–2030.

[17] W. Shan et al., Rigidity-tuning conductive elastomer, Smart Mater. Struct. 24 (2015) 065001.

[18] T. Kaufhold, V. Böhm, K. Zimmermann, Design of a miniaturized locomotion system with variable mechanical compliance based on amoeboid movement, in: IEEE RAS/EMBS Int. Conf. Biomedical Robotics and Biomechatronics, 2012, pp. 1060–1065.

[19] Y. Shan et al., Variable stiffness structures utilizing fluidic flexible matrix composites, J. Intell. Mater. Syst. 20 (2009) 443–456.

[20] S. Somlor, et al., A haptic interface with adjustable stiffness using MR fluid, in: IEEE Int. Conf. Advanced Intelligent Mechatronics, 2015, pp. 1132–1137.

[21] F. Thorsteinsson, I. Gudmundsson, C. Lecomte, Prosthetic and orthotic devices having magnetorheological elastomer spring with controllable stiffness. U.S. Patent 9,078,734 filed 5 Sep. 2012, and issued 14 Jul. 2015.

[22] J.S. Oh et al., A 4-DOF haptic master using ER fluid for minimally invasive surgery system application, Smart Mater. Struct. 22 (2013) 045004.

[23] Y. Li, Y. Maeda, M. Hashimoto, Lightweight, soft variable stiffness gel spats for walking assistance, Int. J. Adv. Robot. Syst. 12 (2015) 175.

[24] L. Wang, F. Iida, Physical connection and disconnection control based on hot-melt adhesives, IEEE-ASME Trans. Mechatron. 18 (2013) 1397–1409.

[25] C. Liu, H. Qin, P.T. Mather, Review of progress in shape-memory polymers, J. Mater. Chem. 17 (2007) 1543–1558.

[26] K. Takashima et al., Pneumatic artificial rubber muscle using shape-memory polymer sheet with embedded electrical heating wire, Smart Mater. Struct. 23 (2014) 125005.

[27] Y. Yang, et al., 3D printing of variable stiffness hyper-redundant robotic arm, in: IEEE Int. Conf. Robotics and Automation, 2016, pp. 3871–3877.

[28] B.E. Schubert, D. Floreano, Variable stiffness material based on rigid low-melting-point-alloy microstructures embedded in soft poly (dimethylsiloxane) (PDMS), RSC Adv. 3 (2013) 24671–24679.

[29] W. Shan, T. Lu, C. Majidi, Soft-matter composites with electrically tunable elastic rigidity, Smart Mater. Struct. 22 (2013) 085005.

[30] C. Mavroidis, Development of advanced actuators using shape memory alloys and electrorheological fluids, Res. Nondestruct. Eval. 14 (2002) 1–32.

[31] M. Sreekumar et al., Critical review of current trends in shape memory alloy actuators for intelligent robots, Ind. Rob. 34 (2007) 285–294.

[32] J.M. Jani et al., A review of shape memory alloy research, applications and opportunities, Mater. Des. 56 (2014) 1078–1113.

[33] S.M. Clarke et al., Anomalous viscoelastic response of nematic elastomers, Phys. Rev. Lett. 86 (2001) 4044–4047.

[34] E. Steltz et al., Jamming as an enabling technology for soft robotics, Proc. SPIE 7642 (2010) 764225.

[35] A.G. Athanassiadis et al., Particle shape effects on the stress response of granular packings, Soft Matter 10 (2014) 48–59.

[36] J.R. Amend et al., A positive pressure universal gripper based on the jamming of granular material, IEEE Trans. Rob. 28 (2012) 341–350.

[37] J.D. Carlson, M.R. Jolly, MR fluid, foam and elastomer devices, Mechatronics 10 (2000) 555–569.

[38] J. de Vicente, D.J. Klingenberg, R. Hidalgo-Alvarez, Magnetorheological fluids: a review, Soft Matter 7 (2011) 3701–3710.

[39] D. Senkal, H. Gurocak, Haptic joystick with hybrid actuator using air muscles and spherical MR-brake, Mechatronics 21 (2011) 951–960.

[40] Z. Varga, G. Filipcsei, M. Zrínyi, Magnetic field sensitive functional elastomers with tuneable elastic modulus, Polymer 47 (2006) 227–233.

[41] K.M. Popp et al., MRE properties under shear and squeeze modes and applications, J. Intell. Mater. Syst. Struct. 21 (15) (2010) 1471–1477.

[42] B.D. Chin, M.S. Chun, H.H. Winter, Modulus-switching viscoelasticity of electrorheological networks, Rheol. Acta 48 (2009) 177–189.

[43] A. Tonazzini, A. Sadeghi, B. Mazzolai, Electrorheological valves for flexible fluidic actuators, Soft Rob. 3 (1) (2016) 34–41.

[44] R. Nava et al., Response time and viscosity of electrorheological fluids, Smart Mater. Struct. 6 (1997) 67–75.

[45] S.K. Chung, H.B. Shin, High-voltage power supply for semi-active suspension system with ER-fluid damper, IEEE Trans. Veh. Technol. 53 (1) (2004) 206–214.

[46] R.T. Bonnecaze, J.F. Brady, Dynamic simulation of an electrorheological fluid, J. Chem. Phys. 96 (3) (1992) 2183–2202.

[47] H. Okuzaki, K. Funasaka, Electromechanical properties of a humido-sensitive conducting polymer film, Macromolecules 33 (2000) 8307–8311.

[48] M. Date, S. Takashita, E. Fukada, et al., Temperature variation of piezoelectric moduli in oriented poly ã-methyl L-glutamate, J. Polym. Sci., Part B: Polym. Phys. 8 (1970) 61–70.

[49] L.E. Faidley, et al., Dynamic response in the low-kHz range and Delta-E effect in ferromagnetic shape memory Ni–Mn–Ga, in: ASME Int. Mechanical Engineering Congress & Exposition (ASME, 2003) IMECE2003-43198.

[50] R.N. Couch, I. Chopra, A quasi-static model for NiMnGa magnetic shape memory alloy, Smart Mater. Struct. 16 (2007) S11–S21.

[51] Z. Yu et al., Large-strain, rigid-to-rigid deformation of bistable electroactive polymers, Appl. Phys. Lett. 95 (19) (2009) 192904.

[52] Y. Feng et al., Biodegradable multiblock copolymers based on oligodepsipeptides with shape-memory properties, Macromol. Biosci. 9 (2009) 45–54.

[53] M.A. McEvoy, N. Correll, Thermoplastic variable stiffness composites with embedded, networked sensing, actuation, and control, J. Compos. Mater. 49 (2015) 1799–1808.

[54] M.C. Yuen, R.A. Bilodeau, R.K. Kramer, Active variable stiffness fibers for multifunctional robotic fabrics, IEEE Robot. Autom. Lett. 1 (2016) 708–715.

[55] H. Koerner et al., Remotely actuated polymer nanocomposites – stress-recovery of carbon-nanotube-filled thermoplastic elastomers, Nat. Mater. 3 (2004) 115–120.

[56] H. Tobushi et al., Thermomechanical constitutive model of shape memory polymer, Mech. Mater. 33 (2001) 545–554.

[57] N. Lagakos et al., Frequency and temperature dependence of elastic moduli of polymers, J. Appl. Phys. 59 (1986) 4017–4031.

[58] A. Firouzeh, M. Salerno, J. Paik, Soft pneumatic actuator with adjustable stiffness layers for multi-dof actuation, in: IEEE/RSJ Int. Conf. Intelligent Robots and Systems, 2015, pp. 1117–1124.

[59] G. McKnight et al., Segmented reinforcement variable stiffness materials for reconfigurable surfaces, J. Intell. Mater. Syst. 21 (2010) 1783–1793.

[60] Y. Chen et al., Variable stiffness property study on shape memory polymer composite tube, Smart Mater. Struct. 21 (2012) 094021.

[61] N. Cheng, et al., Design and analysis of a soft mobile robot composed of multiple thermally activated joints driven by a single actuator, in: IEEE Int. Conf. Robotics and Automation, 2010, pp. 1060–1065.

[62] I.M. Van Meerbeek et al., Foams: morphing metal and elastomer bicontinuous foams for reversible stiffness, shape memory, and self-healing soft machines, Adv. Mater. 28 (14) (2016). 2653-2653.

[63] S. Liang et al., Liquid metal sponges for mechanically durable, all-soft, electrical conductors, J. Mater. Chem. C 5 (7) (2017) 1586–1590.

[64] N.G. Cheng et al., Thermally tunable, self-healing composites for soft robotic applications, Macromol. Mater. Eng. 299 (2014) 1279–1284.

[65] V. Trappe et al., Jamming phase diagram for attractive particles, Nature 411 (2001) 772–775.

[66] N. Cheng, et al., Design and analysis of a robust, low-cost, highly articulated manipulator enabled by jamming of granular media, in: IEEE Int. Conf. Robotics and Automation, 2012, pp. 4328–4333.

[67] N. Cheng et al., Prosthetic jamming terminal device: a case study of untethered soft robotics, Soft Rob. 3 (4) (2016) 205–212.

[68] Y. Wei et al., A novel, variable stiffness robotic gripper based on integrated soft actuating and particle jamming, Soft Rob. 3 (3) (2016) 134–143.

[69] M. Cianchetti et al., Soft robotics technologies to address shortcomings in today's minimally invasive surgery: the STIFF-FLOP approach, Soft Rob. 1 (2) (2014) 122–131.

[70] V. Wall, R. Deimel, O. Brock, Selective stiffening of soft actuators based on jamming, in: IEEE Int. Conf. Robotics and Automation, 2015, pp. 252–257.

[71] Y.J. Kim et al., A novel layer jamming mechanism with tunable stiffness capability for minimally invasive surgery, IEEE Trans. Rob. 29 (4) (2013) 1031–1042.

[72] D. Maruyama et al., Driving force and structural strength evaluation of a flexible mechanical system with a hydrostatic skeleton, J. Zhejiang Univ. Sci. A 11 (2010) 255–262.

[73] S. Sanan, P.S. Lynn, S.T. Griffith, Pneumatic torsional actuators for inflatable robots, J. Mech. Robot. 6 (2014) 031003.

[74] C.M. Best et al., A new soft robot control method, IEEE Rob. Autom. Mag. 23 (3) (2016) 75–84.

[75] R. Qi et al., Design, kinematics, and control of a multijoint soft inflatable arm for human-safe interaction, IEEE Trans. Rob. 33 (3) (2017) 594–609.

[76] R.C. Bell et al., Magnetorheology of submicron diameter iron microwires dispersed in silicone oil, Smart Mater. Struct. 17 (2008) 015028.

[77] J.M. Ginder, L.C. Davis, L.D. Elie, Rheology of magnetorheological fluids: models and measurements, Int. J. Mod. Phys. A 10 (1996) 3293–3303.

[78] L.C. Davis, Model of magnetorheological elastomers, J. Appl. Phys. 85 (6) (1999) 3348–3351.

[79] A. Pettersson et al., Design of a magnetorheological robot gripper for handling of delicate food products with varying shapes, J. Food Eng. 98 (2010) 332–338.

[80] J. Chen, W.H. Liao, Design and control of a magnetorheological actuator for leg exoskeleton, in: IEEE Int. Conf. Robotics and Biomimetics, 2007, pp. 1388–1393.

[81] H. Herr, A. Wilkenfeld, User-adaptive control of a magnetorheological prosthetic knee, Ind. Rob. 30 (1) (2003) 42–55.

[82] C. Majidi, R.J. Wood, Tunable elastic stiffness with microconfined magnetorheological domains at low magnetic field, Appl. Phys. Lett. 97 (16) (2010) 164104.

[83] K.K. Mäkelä, Characterization and performance of electrorheological fluids based on pine oils, J. Intell. Mater. Syst. Struct. 10 (8) (1999) 609–614.

[84] J. Nikitczuk et al., Active knee rehabilitation orthotic device with variable damping characteristics implemented via an electrorheological fluid, IEEE-ASME Trans. Mechatron. 15 (2010) 952–960.

[85] A. Sadeghi, L. Beccai, B. Mazzolai, Innovative soft robots based on electro-rheological fluids, in: IEEE/RSJ Int. Conf. Intelligent Robots and Systems, 2012, pp. 4237–4242.

[86] K. Yoshida, et al., A microgripper using electro-rheological fluid, in: ICCAS-SICE, 2009, pp. 2987–2990.

[87] G.L. Kenaley, M.R. Cutkosky, Electrorheological fluid-based robotic fingers with tactile sensing, in: IEEE Int. Conf. Robotics and Automation, 1989, pp. 132–136.

[88] J.A. Trotter et al., Towards a fibrous composite with dynamically controlled stiffness: lessons from echinoderms, Biochem. Soc. Trans. 28 (2000) 357–362.

[89] L.E. Faidley et al., Modulus increase with magnetic field in ferromagnetic shape memory Ni–Mn–Ga, J. Intell. Mater. Syst. Struct. 17 (2006) 123–131.

[90] T.J. White, D.J. Broer, Programmable and adaptive mechanics with liquid crystal polymer networks and elastomers, Nat. Mater. 14 (2015) 1087–1098.

[91] J. Schätzle, W. Kaufhold, H. Finkelmann, Nematic elastomers: the influence of external mechanical stress on the liquid-crystalline phase behavior, Macromol. Chem. Phys. 190 (1989) 3269–3284.

[92] A. Agrawal et al., Dynamic self-stiffening in liquid crystal elastomers, Nat. Commun. 4 (2013) 1739.

[93] D.M. Agra-Kooijman et al., Dual relaxation and structural changes under uniaxial strain in main-chain smectic-C liquid crystal elastomer, Phys. Chem. Chem. Phys. 17 (2015) 191–199.

[94] W. Hu et al., New dielectric elastomers with variable moduli, Adv. Funct. Mater. 25 (2015) 4827–4836.

[95] S. Rich, S.-H. Jang, Y.-L. Park, C. Majidi, Liquid metal-conductive thermoplastic elastomer integration for low-voltage stiffness tuning, Adv. Mater. Technol. (2017), https://doi.org/10.1002/admt.201700179.

[96] A.M. Nasab et al., A soft gripper with rigidity tunable elastomer strips as ligaments, Soft Rob. (2017), https://doi.org/10.1089/soro.2016.0039 (in press).

[97] W.L. Shan et al., Thermal analysis and design of a multi-layered rigidity tunable composite, Int. J. Heat Mass Transf. 66 (2013) 271–278.

[98] Z. Ren et al., Phase-changing bistable electroactive polymer exhibiting sharp rigid-to-rubbery transition, Macromolecules 49 (2016) 134–140.

[99] U.G.K. Wegst et al., Bioinspired structural materials, Nat. Mater. 14 (2015) 23–36.

[100] X. Wang, Y. Mei, M.Y. Wang, Level-set method for design of multi-phase elastic and thermoelastic materials, Int. J. Mech. Mater. Design 1 (2004) 213–239.

[101] M. Behl, A. Lendlein, Shape-memory polymers, Mater. Today 10 (2007) 20–28.

[102] P.T. Mather, X. Luo, I.A. Rousseau, Shape memory polymer research, Annu. Rev. Mater. Res. 39 (2009) 445–471.

[103] H. Meng, G. Li, A review of stimuli-responsive shape memory polymer composites, Polymer 54 (2013) 2199–2221.

[104] T.C. Halsey, Electrorheological fluids, Science 258 (1992) 761–766.

[105] V. Kafka, Shape memory polymers: a mesoscale model of the internal mechanism leading to the SM phenomena, Int. J. Plast 24 (2008) 1533–1548.